Modulation of Cellular Apoptosis with Apoptotic Protease-Activating Factor 1 (Apaf-1) Inhibitors

L. Mondragón,[†] M. Orzáez,[†] G. Sanclimens,[‡] A. Moure,[‡] A. Armiñán,[§] P. Sepúlveda,[⊥,§] A. Messeguer,[‡] M. J. Vicent,*[,†] and E. Pérez-Payá*[,#]

Department of Medicinal Chemistry, Centro de Investigación Príncipe Felipe, Valencia, Spain, Department of Biological Organic Chemistry, IIQAB, CSIC, Barcelona, Spain, Cardioregeneration Unit, Centro de Investigación Príncipe Felipe, Valencia, Spain, Fundación Hospital General Universitario de Valencia, Consorcio Hospital General Universitario de Valencia, Valencia, Spain, and Instituto de Biomedicina de Valencia, CSIC, Valencia, Spain

The programmed cell death or apoptosis plays both physiological and pathological roles in biology. Anomalous activation of apoptosis has been associated with malignancies. The intrinsic mitochondrial pathway of apoptosis activation occurs through a multiprotein complex named the apoptosome. We have discovered molecules that bind to a central protein component of the apoptosome, Apaf-1, and inhibits its activity. These new first-in-class apoptosome inhibitors have been further improved by modifications directed to enhance their cellular penetration to yield compounds that decrease cell death, both in cellular models of apoptosis and in neonatal rat cardiomyocytes under hypoxic conditions.

Introduction

Apoptosis is a fundamental mechanism of programmed cell death that is regulated physiologically and genetically and plays a central role in development, normal cell turnover, and immune system function. Moreover, abnormal apoptotic processes are important and influence the severity of disease progression in a number of pathologies. Defects in appropriate suppression of apoptosis are observed in cancer pathogenesis[1] and autoimmune disorders,[2] while anomalous induced apoptosis plays an important role in acquired immunodeficiency disease (AIDS),[3] and neurodegenerative and heart diseases.[4,5] The mechanism of apoptosis is executed by a family of highly conserved proteases known as caspases,[6] which in a cascade of sequential initiator and effector members dismantle the cell. Different cell death stimuli can initiate the mechanism. In particular, defined apoptotic signals activate the mitochondria-mediated or intrinsic pathway that utilizes caspase-9 as its initiator. Caspase-9 activation is triggered by the release to the cytoplasm of proapoptotic proteins from the mitochondrial intermembrane space, in particular cytochrome *c* and Smac/Diablo.[7,8] The formation of the macromolecular complex named apoptosome is a key event in this pathway. The apoptosome is a holoenzyme multiprotein complex formed by cytochrome *c* activated Apaf-1[a] (apoptosis protease-activating factor), dATP, and procaspase-9.[9] Understanding the mechanisms of functional activation of the apoptosome has helped to define prospective targets for treating deregulated apoptosis that is associated with human pathologies.[10] However, inappropriate apoptosome activity has been shown to play a role in neurodegenerative disorders and

its suppression by biological tools provided resistance to apoptosis induction.[11,12] Inactivation of the apoptosome might provide a therapeutic avenue for treating not only neurodegenerative but other diseases such as ischemia and cardiac and renal failure.

We have early developed a new structural class of Apaf-1 ligands as apoptosome inhibitors.[13] From this family of *N*-alkylglycine inhibitors, the most potent in vitro was peptoid **1** (Chart 1). However, this hit exhibited low membrane permeability and modest efficacy arresting apoptosis in cells. We have shown that fusion of peptoid **1** to known cell penetrating peptides[14] facilitates cell permeation in defined cellular models of apoptosis. Furthermore, the conjugation of peptoid **1** to a polymeric carrier (PGA−**1**) demonstrated an enhanced efficacy probably related to an efficient lysosomotropic drug release on the cytosol.[15] Here, we have extended these studies by exploring the activity of PGA−**1** in different cellular models of apoptosis, such as human cervix adenocarcinoma (HeLa), human histiocytic lymphoma (U937), human osteosarcoma (U-2 OS), human lung carcinoma (A549), and human osteogenic Sarcoma (Saos-2) with inducible expression of Bax. In addition, we have also explored how restriction of the conformational mobility of peptoid **1** through backbone cyclization decreased the unspecific toxicity of **1** and increased its antiapoptotic activity. A systematic comparative study of these new first-in-class apoptosome inhibitors has been developed, and the results suggested that inhibition of the apoptosome resulted in increased cell recovery, when compared to control cells, after the apoptotic insult. Finally, we carried out studies directed to explore the use of apoptosome inhibitors as agents that could decrease the degree of apoptosis in neonatal rat cardiomyocytes subjected to hypoxic conditions.

Results and Discussion

To increase the cellular activity of the originally identified apoptosome inhibitor peptoid **1**,[13] structural modifications of

---

* To whom correspondence should be addressed. For M.J.V.: phone, +34-963289680; fax, +34-963289701; e-mail, mjvicent@cipf.es. For E.P.-P.: address, Centro de Investigación Príncipe Felipe, Av. Autopista del Saler, 16, E-46013 Valencia, Spain; phone, +34-963289680; fax, +34-963289701; e-mail, eperez@cipf.es.

† Department of Medicinal Chemistry, Centro de Investigación Príncipe Felipe.

‡ IIQAB, CSIC.

§ Cardioregeneration Unit, Centro de Investigación Príncipe Felipe.

⊥ Consorcio Hospital General Universitario de Valencia.

Instituto de Biomedicina de Valencia, CSIC.

[a] Abbreviations: Apaf-1, apoptotic protease-activating factor; DEVDase, hydrolysis of Ac-DEVD-afc peptide; DTT, dithiothreitol; FCS, fetal-calf serum; MEFs, mouse embryo fibroblasts; MMP, mitochondrial membrane potential; MTT, 3-(4,5-dimethylthiazol-2-yl)-2,5-diphenyltetrazolium bromide; Ni-NTA, (Ni^{2+} nitrilotriacetate)–agarose; PBS, phosphate buffered saline; PGA, poly-L-glutamic acid); rApaf-1, recombinant Apaf-1.

Chart 1. Chemical Structure of **1** and Its Derivatives Studied Here, Namely, Peptide−Peptoid Hybrids (As Example, PEN−**1**[a]), PGA−peptoid Conjugate, and the Cyclic Derivative, **2**

1 **PEN-1** **PGA-peptoid conjugate (PGA-1)** **2**
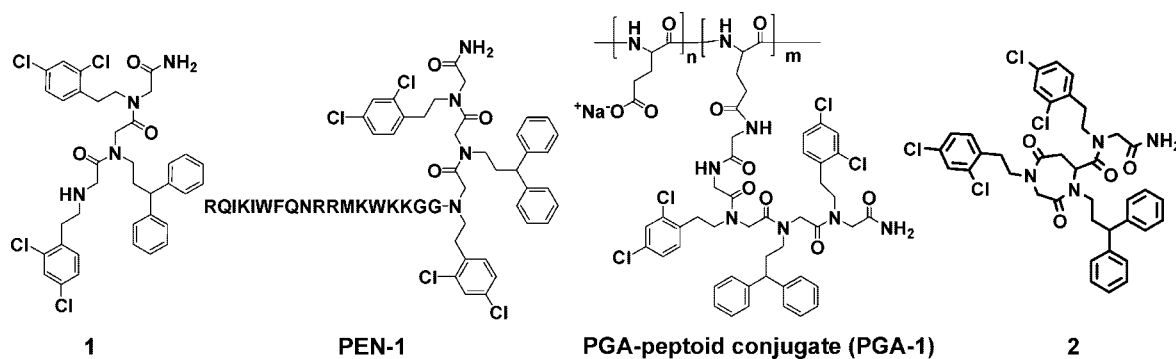
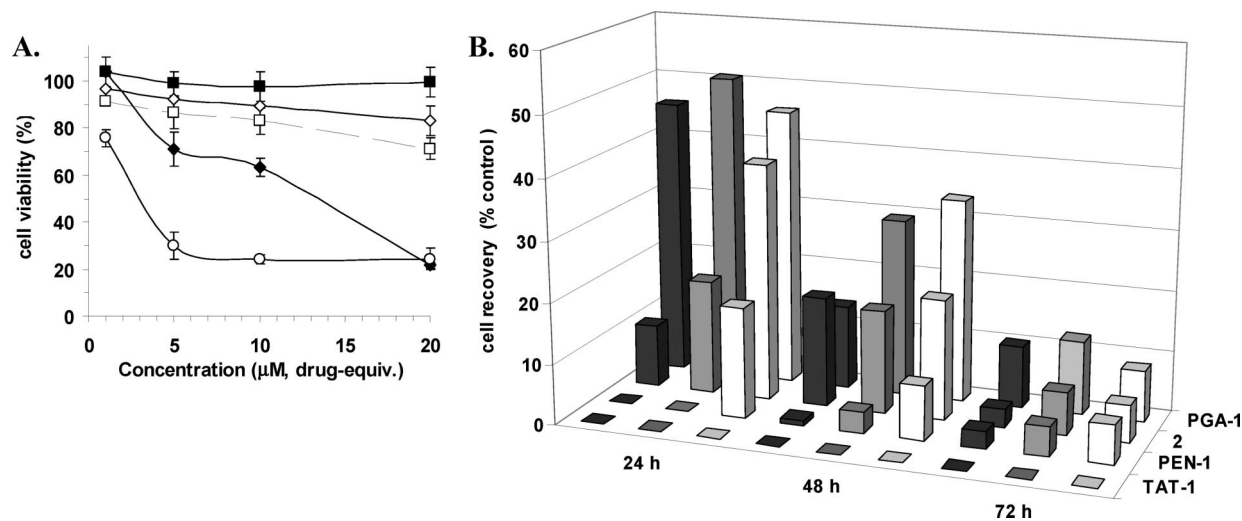[a] One-letter code for the amino acids has been used to describe the peptidic part of the molecule.

Figure 1. MTT cell viability measurements of peptoid **1** derivatives. (A) Cytotoxicity of peptoid **1** (◆), the different peptide/peptoid hybrids (□ PEN−**1** and ○ TAT−**1**), compound **2** (◇), and PGA−**1** (■) against U937 cells measured after 24 h of incubation. Data are expressed as the mean ± SE ($n > 3$). (B) Evaluation of compound-dependent cell recovery after doxorubicin-induced cell death in U-2 OS cells. The peptoid derivatives and compound **2** were evaluated at different concentrations (10, 5, and 1 μM (black, gray, and white bars, respectively)) after 24, 48, and 72 h of incubation. In all cases, SE < 10%. Data are expressed as the mean ± SE ($n > 3$).

this compound had to be done because of its poor solubility and low membrane permeability. The potential production of undesirable side effects due to the conformational freedom of peptoids was also a matter of concern. Thus, we focused our studies on delivery systems by means of adequate carriers or on chemical modifications that could diminish the conformational mobility of peptoid **1**. These goals were addressed in three different ways: (i) by the design of hybrid peptide/peptoid conjugates where the parent peptoid **1** was fused to well characterized cell penetrating peptides (CPPs) such as penetratin (PEN) and Tat HIV-1 (TAT) peptides, yielding compounds PEN−**1** and TAT−**1**,[14] respectively; (ii) by means of backbone cyclization; (iii) by conjugation to a water soluble polymeric carrier such as poly-L-glutamic acid (PGA), obtaining PGA−peptoid conjugates.[15]

Cytotoxicity and Cell Recovery Capability of Peptoid 1 Derivatives. Before proceeding with cellular models of apoptosis inhibition, the unspecific toxicity of the compounds in our cell panel was analyzed by means of MTT assays (see Experimental Section for full details on cell lines) (Figure 1A).

TAT−**1** and PEN−**1** were found to be highly and slightly toxic, respectively, for the cells. In contrast, both **2** and PGA−**1** were shown to be devoid of unspecific cell toxicity. The

enhancement of peptoid **1** cytotoxicity after fusion with TAT peptide could be related to a cargo-induced restriction of the conformational space available for the CPPs that could be necessary for an effective and safe cellular membrane permeation.[14] A preliminary analysis of the antiapoptotic activity of peptoid **1** derivatives was performed in osteosarcoma U-2 OS cells where the cytotoxic compound doxorubicin induces cell death in a time and concentration dependent manner. Doxorubicin induces apoptosis through DNA damage that is transduced to the mitochondria, disturbing the mitochondrial membrane potential (MMP) and activating executioner caspases through involvement of the apoptosome. After 12 h, 2 μM doxorubicin-treated cells demonstrated staining for annexin V-PE (which specifically binds to exposed phosphatidylserine) and loss of MMP, both being feature markers of an apoptotic cellular phenotype.[13] When cells were treated with doxorubicin in the presence of **2** and PGA−**1**, the extent of apoptosis was remarkably diminished as determined by the lowered percentage of cells showing apoptotic phenotype (Figure 1B). In contrast, as expected from the previous unspecific cell toxicity evaluation, TAT−**1** did not prevent cellular death and PEN−**1** showed only partial protection at low concentration, evidencing a compromise between the protective effect of the peptoid **1** and residual
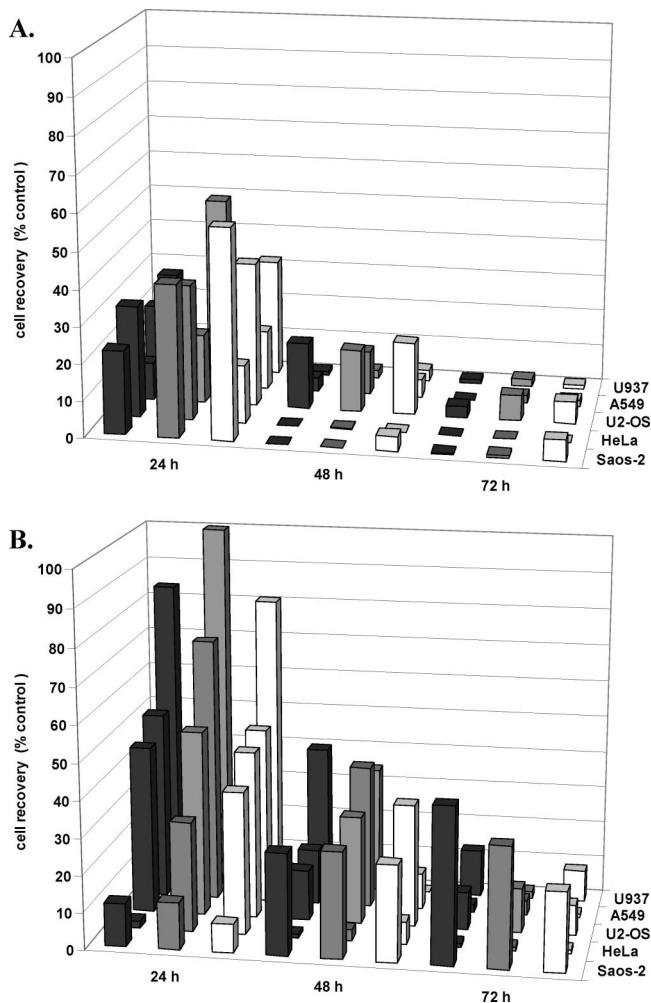
A.

B.

Figure 2. Evaluation of cell death inhibition in different cell lines by **2** (A) and PGA−**1** (B). **2** was evaluated at 10, 5, and 1 μM (black, gray, and white bars, respectively) and PGA−**1** at 100, 50, and 20 μM drug equivalent (black, gray, and white bars, respectively) after 24, 48, and 72 h of incubation. Data are expressed as the mean $\pm$ SE ($n >$ 3). In all cases, SE < 10%.

unspecific toxicity associated with the whole molecule (Figure 1B). Compound **2** and PGA−**1** were then selected for a systematic study as cell death inhibitors using different cell lines and different cell death inducers.

To prove the extent of protection against apoptosis of compounds **2** and PGA−**1**, they were evaluated in a panel of different cell models (U937 histiocytic lymphoma, A549 lung carcinoma, HeLa adenocarcinoma, and U-2 OS osteosarcoma) using doxorubicin as apoptosis inducer. In addition, we also evaluated a more well defined model of "only intrinsic" apoptosis using Saos-2 cells were apoptosis is induced by the doxycyclin-dependent conditional expression of Bax through the tet-ON system (Clontech). Bax is a proapoptotic member of the Bcl-2 family that induces apoptosis by the release of cytochrome *c* from the mitochondria;[16,17] thus, activation of apoptosis solely relies on the mitochondrial pathway. Figure 2 summarizes the cell death inhibitory activity of **2** (Figure 2A) and PGA−**1** (Figure 2B) in the above-mentioned cell panel.

The two compounds, **2** and PGA−**1**, substantially decreased apoptosis in both doxorubicin-induced (U937, U-2 OS, HeLa, and A549 cell lines) and doxycyclin-induced (Saos-2 cells) cell death when cell viability was evaluated at 24 h after treatment (up to 60% of cell death inhibition in the Saos-2 cell line was obtained when using a 1 μM **2** ($p < 0.001$) and up to 100% in

the U937 cell line when a 50 μM drug equivalent of PGA−**1** was used ($p < 0.05$)). It is important to note that PGA conjugates (i.e., like the PGA−**1** analyzed in the present study) are usually active at concentrations 10-fold higher than the parent low molecular weight drugs because of the different pharmacokinetics.[18]

It is well established that inhibition of apoptotic cell death should correlate with inhibition of executioner caspases. Then we were willing to evaluate caspase-3 activity in extracts derived from cells that were treated with both the apoptosis inducer and the inhibitors and compare the results to those obtained from cell extracts only treated with the inducers (Figure 3). Initially, the compounds PEN−**1**, **2**, and PGA−**1** were evaluated in a common cell line, Saos-2. At this point, for comparative purposes, we decided to include in our study the diarylurea-based compound **3** previously described as apoptosome inhibitor.[19] PEN−**1** and **3** showed low caspase-3 inhibitory activity in these experimental conditions. However, the inhibition of the apoptosome activity by the treatment of the cells with **2** and PGA−**1** resulted in inhibition of caspase-3 activity. **2** was effective when the cell extract was obtained after 24 h of treatment, while PGA−**1** showed increased activity at longer times ($p < 0.001$) (Figure 3A). The delay on time to reach the activity obtained for PGA−**1** when compared to **2** is probably due to the mechanism of action and cellular pharmacokinetics of polymeric drugs. Effective biological activity of polymer−drug conjugates relies on lysosomal enzyme cleavage to release active drug in a specific place after cellular uptake by endocytosis.[15] Interestingly, PGA−**1** reaches values up to 100% of caspase-3 inhibition at 50 μM drug equivalent (HeLa at 48 h and Saos-2 at 72 h) ($p < 0.05$) (Figure 3B), whereas **2** at 5 μM reaches inhibitory percentages of 50−60% (U-2 OS at 48 h and HeLa at 48 h, respectively) ($p < 0.05$) (Figure 3C). The good correlation found in our analysis of caspase-3 inhibition and cell recovery could suggest that the compounds are direct inhibitors of the enzymatic activity of caspase-3; however, this is not the case. In fact, none of the compounds here analyzed was able to inhibit caspase-3 using a recombinant-protein based assay (results not shown). In contrast, when we directly activated the apoptosome with an apoptosome activator (compound **4**) recently described by Nguyen and Wells,[20] we obtained cell protection when **4** was provided to the cells in the presence of the apoptosome inhibitor PGA−**1** ($p < 0.001$) (Figure 3D).

Compound 2 Analogues. As explained above, the cyclic derivative **2** was one of the most active peptoid **1** derivatives together with PGA−**1** conjugate. In order to seek further optimization, several structural modifications of **2** were carried out. Initially we focused our attention on the 2′,4′-dichlorophenylethyl substituent attached to the perhydro-1,4-diazepine-2,5-dione ring (**I**, Chart 2). This substituent turned out to be essential for activity, and in our hands, any attempt at modification resulted in a loss of antiapoptotic activity. Similar results were found in early attempts at modification of the 3,3-diphenylpropyl moiety.[13] Then we addressed our attention to the R$_1$ moiety. As shown in Table 1, a series of 8 derivatives (**2a−h**) were designed and their preparation was carried out by using a practical approach. Thus, according both to the nature of the R$_1$ moiety and to the expected behavior of the mixtures in preparative HPLC, these analogues were separated into three subsets containing two, three, and three compounds (**2a** and **2b**, **2c−e**, and **2f−h**, respectively). Then each subset of compounds was prepared by using a synthetic pathway based on solid-phase and microwave activation and using the positional scanning approach for construction of controlled mixtures. By
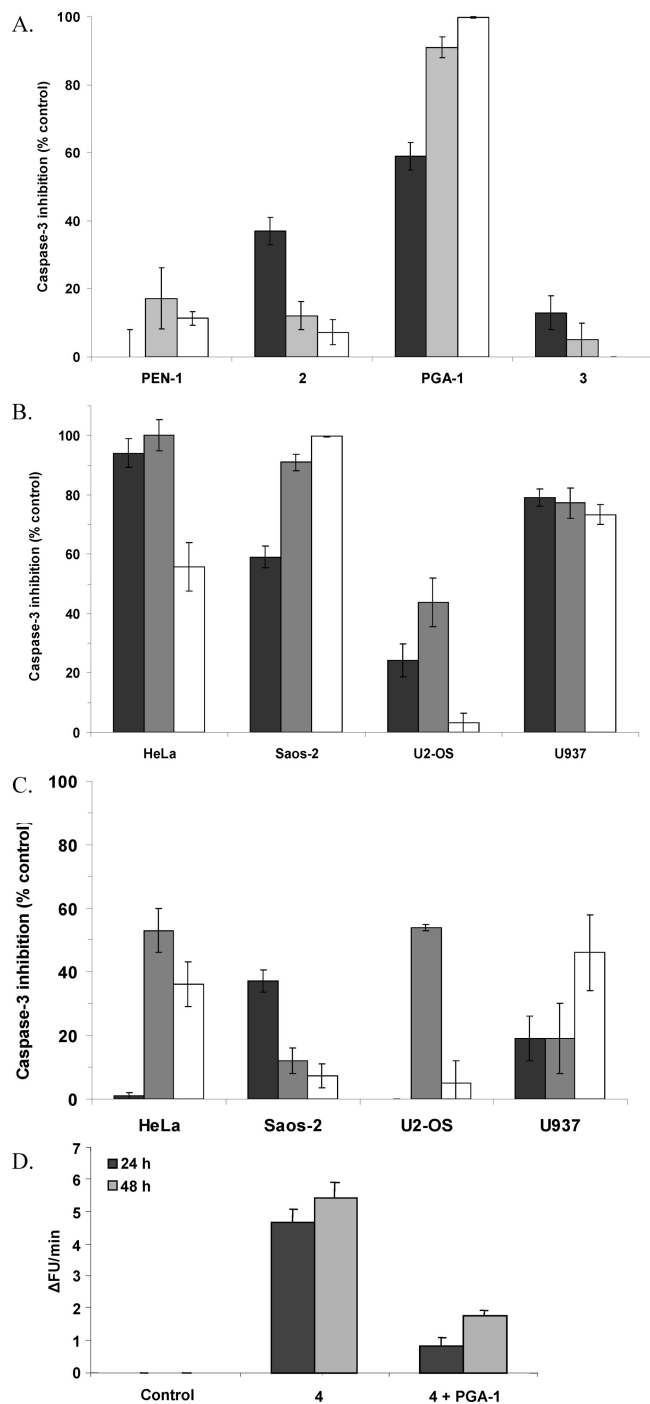
Figure 3. Caspase-3 (C3) activity in cell extracts measured by the fluorimetric DEVDase assay at 24, 48, and 72 h incubation times (black, gray, and white bars, respectively): (A) comparison of C3 activity in Saos-2 cell extracts after incubation with the different peptoid **1** derivatives (all compounds at 5 μM concentration except PGA−**1**, which was used at 50 μM drug equivalent); C3 activity in different cell lines after incubation with PGA−**1** at 50 μM drug equivalent (B) and **2** at 5 μM concentration (C); (D) C3 activity in U-937 cells after direct activation of the apoptosome assembly[20] with compound **4** in the presence and absence of PGA−**1** at 50 μM drug equivalent. Data are expressed as the mean ± SE (n > 3).

this procedure, three HPLC purifications were only required for isolating all compounds in purities over 98% and satisfactory overall yields.

Table 1 summarizes the caspase-3 inhibitory activity determined in cell extracts and the observed cell recovery when apoptosis was induced in Saos-2 cells upon treatment with

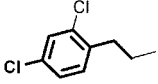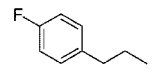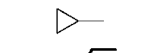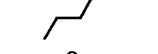**Chart 2.** Chemical Structure of **2** and Its Derivatives Here Studied
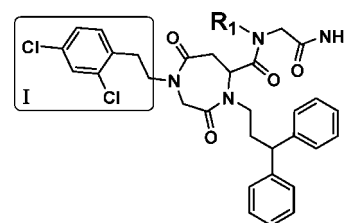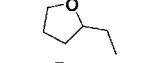
doxycyclin, in the presence or absence of the compound subjected to evaluation. As expected from previous results, replacement of the 2′,4′-dichlorophenylethyl moiety at R_1 by a nonaromatic moiety resulted in a decrease of potency (compounds **2c**, **2d**, **2e**, **2g**). However, the behavior of compound **2c** was a bit off provided that the inhibition of caspase-3 activity was systematically close to 50% while the cell recovery ability was 2%. Also, the activity in the cell recovery experiment for this compound was slightly higher at 1 μM (not shown) than at 5 μM. It is mentioned that in certain occasions, biological assays developed with cell extracts and whole cell systems provide results that 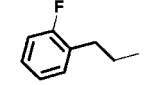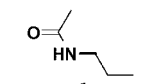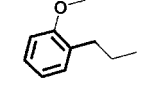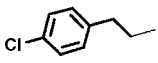are more difficult to rationalize when compared to those obtained from in vitro experiments. Furthermore, parallel studies to analyze the unspecific toxicity of the compounds suggested that only compound **2d** was toxic. Different electronegative atoms (such as O or F) in several positions (para, meta, or ortho) were also used in order to evaluate the effect of the electronic density changes on this family of apoptosome inhibitors (namely, **2a**, **2e**, **2g**, and **2h**). In general, although all these analogues exhibited the capability of reducing the apoptosis induced in Saos-2 cell line, none of them showed a significant improvement when compared to compound **2**. Similar results were obtained in the other models of our cell panel mentioned above (HeLa, A549, U-2 OS, and U-937 cells; data not shown). Taken altogether, it is not easy to make an appropriate SAR because no clear trend was obtained. However, it would be possible to suggest that the presence of a second 2′,4′-dichlorophenylethyl substituent is not essential but important for the activity, probably because of the presence of the two electronegative atoms and, certainly, of the aromatic ring. This is still an ongoing research, and new efforts are currently being devoted to modify the 1,3-diphenylpropyl substituent as well as to explore other heterocyclic scaffolds.

Membrane Potential Recovery after PGA−1 Treatment. Mitochondria play a prominent role in cell death as a central organelle involved in the signal transduction and amplification of the apoptotic response.[21,22] Mitochondrial dysfunction is an early event characterized by an increase in mitochondrial membrane permeability. Thus, cells undergoing apoptosis are characterized by a low mitochondrial membrane potential ($\Delta\Psi_m^{low}$). In fact, when Saos-2 and U937 cells were subjected to an apoptotic insult (Saos-2 treated with doxycycline and U937 with doxorubicin), the number of cells with $\Delta\Psi_m^{low}$ increased when compared to untreated cells (p < 0.05) (Figure 4). However, the effect was clearly attenuated when cells were subjected to the insult in the presence of PGA−**1**. This result suggests that PGA−**1** treated cells could probably overcome apoptosis at this postmitochondrial level of the pathway. Although still speculative, this class of compounds could inhibit processes downstream from the mitochondrial depolarization event. Then damaged cells, at early stages of depolarization, could still be in a reversible step of the apoptotic process, and inhibition of Apaf-1 could result in a recovery of mitochondrial potential. Another possibility is that the recovery of membrane

Table 1. Percentage of Cell Recovery and Inhibition of Caspase-3 Activity Obtained with Compound **2** Analogues in Bax-Induced Apoptosis in Saos-2 Cell Line[a]

Compound 2 analogues	R₁	Cell recovery assay (%)[a]	Caspase-3 inhibition assay (%)[a]
2		50 ± 3	53 ± 4
2a		57 ± 18	34 ± 8
2b		10 ± 6	16 ± 11
2c		2 ± 1	45 ± 5
2d		9 ± 5	ND
2e		16 ± 8	51 ± 5
2f		12 ± 6	21 ± 9
2g		41 ± 12	1 ± 1
2h		23 ± 10	2 ± 1

[a] Cell recovery and caspase-3 activity were analyzed after 24 h of treatment with the respective compounds at 5 μM concentration. Data are expressed as the mean $\pm$ SE ($n > 3$). ND: not determined.
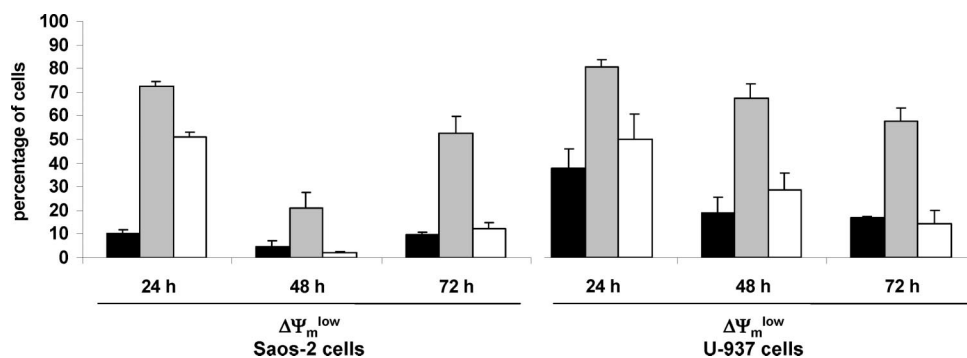

Figure 4. Evaluation of apoptosis by flow cytometry as the percentage of cells with low membrane potential ($\Delta\Psi_m^{low}$): flow cytometry analysis of $\Delta\Psi_m$ of Saos-2 and U-937 cells untreated (black bars); subjected to an apoptotic insult by treatment with doxycyclin and doxorubicin, respectively (gray bars); when the apoptotic insult was applied in the presence of PGA−1 at 50 μM drug equivalent (white bars). Data are expressed as the mean $\pm$ SE ($n > 3$).

potential of the population would be related to a process downstream from the mitochondria, such as the loss or not of plasmatic membrane potential caused by a decrease in the intracellular levels of K$^+$ ions. Although the ability of mitochondrial recovery after partial depolarization is still a matter of discussion, it seems well accepted that it could occur in neurons,[23] but it is controversial in other cell types as smooth muscle cells or myofibroblasts.[24]

Inhibition of Hypoxia-Induced Apoptosis in Primary Culture Cardiomyocytes by PGA−1. Apoptosis plays a crucial role in ischemic-based diseases. Among them, myocardial damage induced by ischemia−reperfusion has been shown to be directly associated with apoptosis. Furthermore, after myocardial infarction, the presence of apoptotic cells has been demonstrated both in the infarct area and in the border zone of the infarction.[25−30] Although the signal transduction pathways are not completely defined, it is known that mitochondrial

dysfunction is one of the most critical events associated with myocardial ischemia−reperfusion injury.[31,32] In this sense, previous studies showed that very low levels of cardiac myocyte apoptosis are sufficient to produce heart failure.[33] In addition, reduction of myocyte apoptosis by the potent polycaspase inhibitor IDN-1965 improved left ventricular function and survival of mice with an induced peripartum cardiomyopathy.[34] We therefore analyzed the ability of the apoptosome inhibitors here described, and in particular PGA−1, as potential inhibitors of hypoxia-induced apoptosis in cardiomyocytes with an ex vivo model of myocardial infarction. Then primary cultures of neonatal rat cardiomyocytes were established and subjected to hypoxic conditions. A double immunohistochemistry based procedure clearly showed the presence of apoptotic cells and active caspase-3 demonstrating the active role of apoptosis in hypoxia-induced cardiomyocytes cell death (Figure 5A). The presence of Apaf-1 protein in neonatal cardiomyocytes was also
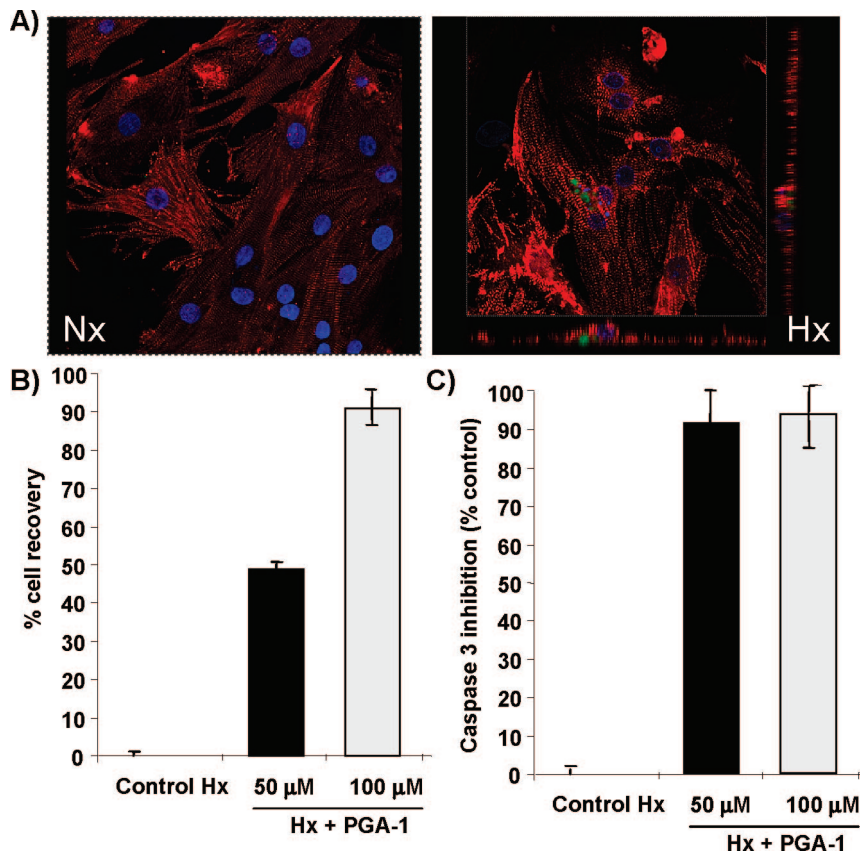
Figure 5. PGA−1 is capable of reducing hypoxia-induced apoptosis in primary culture cardiomyocytes. (A) Apoptosis induction in primary culture cardiomyocytes subjected to hypoxia. Double immunohistochemistry of cardiomyocytes with anti-caspase 3 (green) and anti-α-actinine (red) antibodies was analyzed by confocal microscopy (40× magnification). Nuclei are stained with DAPI (blue). (B) Evaluation of induced cell death inhibition by MTT assay, showing PGA−1 at different concentrations (50 and 100 μM drug equivalent; black and gray, respectively) after 24 h of incubation. (C) Caspase-3 activity in cell extracts measured by the fluorimetric DEVDase assay at 24 h of incubation time. Data are expressed as the mean ± SE ($n > 3$).

determined by Western blot (data not shown). These results provide a validation of the cellular model selected for our ex vivo studies. Importantly, when the neonatal cardiomyocytes were subjected to the hypoxia conditions in the presence of PGA−1, the percentage of cell death was clearly diminished when compared to the control cell population ($p < 0.05$) (Figure 5B). Furthermore, to determine whether or not PGA−1 could decrease caspase-3 activity in this cell system, cells from a 2-day-old established culture were subjected to the hypoxia conditions in the presence of different concentrations of PGA−1 and caspase-3 activity was assessed (Figure 5C). The results revealed a marked PGA−1 dependent decrease of caspase-3 activity ($p < 0.001$).

Conclusions

The overall data obtained suggest that apoptosome inhibitors can decrease the extension of cell death. Two important concepts come into view from this study. First, compound **2** and the PGA-based derivative PGA−1 inhibit apoptosis in different cell lines. Second, inhibition of the intrinsic cell death (or mitochondrial) pathway by specific inhibition of Apaf-1 could result in the recovery of the cells or in prevention of the cellular damage induced by apoptotic insults. Whether or not this could have therapeutic interest is a fundamental question. In this sense, we have observed that PGA−1 was active inhibiting hypoxia-induced cell death in cardiomyocytes. Although the results shown here are derived from ex vivo studies, we are now moving ahead to the next level of complexity that represents

an appropriate in vivo model. We are currently evaluating different experimental models of myocardial infarction. If the compounds analyzed here further demonstrate the ability to reduce hypoxia-induced cardiomyocyte apoptosis in vivo, it would result in a prevention of ventricular remodeling and improvement of damaged cardiac function. That in turn would open new strategies to improve the therapeutic resources for the treatment of this unfortunately very common pathology.

Experimental Section

Materials. Poly-L-glutamic acid sodium salt (PGA), *N,N*-diisopropylcarbodiimide (DIC), 1-hydroxybenzotriazole (HOBt), diisopropylethylamine (DIEA), and anhydrous dimethylformamide (DMF) were purchased from Sigma-Aldrich and used without further purification. All solvents including HPLC grade were obtained from Merck (Barcelona, Spain). Tissue culture grade dimethylsulfoxide (DMSO), 3-(4,5-dimethylthiazol-2-yl)-2,5-diphenyltetrazolium bromide (MTT), trypan blue solution (0.4%) (cell culture grade), bovine cathepsin B, and dithiothreitol (DTT) were from Sigma-Aldrich. Samples of 0.25% trypsin−EDTA, fetal calf serum (FCS), RPMI 1640 with L-glutamine, D-MEM with L-glutamine, and collagenase type II were from Gibco BRL Life Technologies (Paisley, U.K.). Annexin V-FITC apoptosis detection kit I was from BD PharmingenTM (BD Bioscience, Madrid, Spain) and 3,3′-dihexyloxacarbocyanine iodide (DIOC$_6$(3)) from Molecular Probes (Invitrogen, Barcelona, Spain). The fluorogenic caspase-3 substrate, Ac-DEVD-afc, was purchased from Biomol International LP (Exeter, U.K.). Protein quantification was performed with a bicinchoninic acid kit from Pierce Technology Corporation (NJ). Dispase was purchased from Roche Diagnostics (Godo Shusei Co,

Ltd., Tokyo, Japan). For immunochemistry assays, rabbit polyclonal active caspase-3 antibody was purchased from Cell Signaling Technology (Beverly, MA) and mouse monoclonal anti-α-actinine (sarcomeric) was purchased from Sigma-Aldrich. Antirabbit and antimouse secondary antibodies were coupled to FITC and cyanine-3, respectively, and were purchased from Jackson Immunoresearch (Suffolk, England). All other reagents were of general laboratory grade.

Chemistry. The HPLC analyses of peptoid **1** and compound **2** and its analogues were carried out with a Hewlett-Packard series 1100 (UV detector 1315A) modular system using a Kromasil 100 C8 (15 cm × 0.46 cm, 5 μm) column with CH_3CN-H_2O mixtures containing 0.1% TFA at 1 mL/min as mobile phase and with monitoring at 220 nm. Compounds were purified from the crude reaction mixture by semipreparative HPLC using a Kromasil C8 (25 cm × 2 cm, 5 μm) column, CH_3CN-H_2O mixtures containing 0.1% TFA as mobile phases, and a flow rate of 5 mL/min. The NMR spectra of peptoids were recorded in CD_3OD solutions using a Varian Inova 500 apparatus (^{1}H NMR, 500 MHz; ^{13}C NMR, 125 MHz). The assignments of absorptions observed for peptoid **1** and compound **2** were confirmed by gDQCOSY and gHSQC experiments. The different conformations present in both compounds led to the observation of complex absorptions. High-resolution mass spectra (HRMS-FAB) were carried out at the Mass Spectrometry Service of the University of Santiago de Compostela (Spain). The synthesis and characterization of PGA−**1**, PEN−**1**, and TAT−**1** have been reported.[14,15]

Synthesis of [*N*-(2,4-Dichlorophenethyl)glycyl]-[*N*-(3,3-diphenylpropyl)]glycyl]-*N*-(2,4-dichlorophenethyl)glycinamide (1). The synthesis of this peptoid was carried out following the method described elsewhere.[35] ^{1}H NMR: δ 7.5–7.4 (2H, CH$_{Ar}$), 7.25–7.35 (12H, CH$_{Ar}$), 7.15 (2H, CH$_{Ar}$), 4.2–3.8 (6H, COCH$_2$N), 4.02 (1H, CH), 3.58 (2H, NCH$_2$), 3.20 (2H, NCH$_2$CH), 3.15 (2H, NHCH$_2$), 3.10 (2H, NHCH$_2$CH$_2$), 3.0–2.90 (2H, NCH$_2$CH$_2$), 2.4–2.1 (2H, NCH$_2$CH$_2$CH). ^{13}C NMR: δ 172.62, 172.39 (CO), 170.14, 169.87 (CO), 167.53, 166.60 (CO), 145.85 (2 × C$_{Ar}$), 136.0 (2 × C$_{Ar}$), 134.2 (2 × C$_{Ar}$), 133.8 (2 × C$_{Ar}$), 133.2, 133.1 (2 × CH$_{Ar}$), 129.8 (2 × CH$_{Ar}$), 129.5 (2 × CH$_{Ar}$), 128.9 (4 × CH$_{Ar}$), 128.8 (4 × CH$_{Ar}$), 127.4 (2 × CH$_{Ar}$), 50.4 (COCH$_2$N), 49.5 (CH), 49.1 (NCH$_2$), 48.9 (COCH$_2$N), 48.2 (NCH$_2$CH), 48.1 (COCH$_2$N), 47.8 (HNCH$_2$), 34.2 (NCH$_2$CH$_2$CH), 32.6 (NCH$_2$CH$_2$), 30.4 (HNCH$_2$CH$_2$). HRMS (M + 1) calcd C$_{37}$H$_{39}$^{35}Cl$_4$N$_4$O$_3$, 727.1747; found, 727.1751.

Synthesis of 1-(3′,3′-Diphenylpropyl)-4-[2′-(2″,4″-dichlorophenyl)ethyl]-7-[*N*-aminocarbonylmethyl-*N*-[2′-(2″,4″-dichlorophenyl)ethyl]aminocarbonyl]perhydro-1,4-diazepine-2,5-dione (2). The synthesis of this heterocyclic derivative was carried out following a solid-phase general procedure with microwave activation developed in our laboratory that is briefly described below for the preparation of compound **2** analogues and that will be reported elsewhere. ^{1}H NMR: δ 7.62–7.53 (2H), 7.48–7.35 (2H), 7.32–7.23 (10H), 7.16 (m, 2H), 4.70, 4.60 (1H, (CH)$_{het}$), 4.21, 4.19 (d, J = 17.1 Hz, 1H, (COCH$_2$N)$_{het}$), 4.02–3.78 (1H (COCH$_2$N)$_{het}$ + 2H (COCH$_2$N) + 1H (CH)), 4.02 (CHPh$_2$), 3.53–3.45 (6H, NCH$_2$), 3.00, 293 (dd, J = 14.7 and 6.3 Hz, 1H, COCH$_2$CH), 2.90–2.71 (5H, 1H (COCH$_2$CH) + 4H(NCH$_2$CH$_2$)), 2.48–2.15 (2H, NCH$_2$CH$_2$CH). ^{13}C NMR: δ 172.5 (CO), 171.5, 170.8 (CO), 170.1 (CO), 169.3 (CO), 145.4 (C$_{Ar}$), 145.0 (C$_{Ar}$), 136.3–135.4 (2 × C$_{Ar}$), 134.7 (2 × C$_{Ar}$), 133.5 (CH$_{Ar}$), 133.1 (CH$_{Ar}$), 132.9 (CH$_{Ar}$), 132.5 (2 × C$_{Ar}$), 129.4–129.0 (4 × CH$_{Ar}$), 128.1 (4 × CH$_{Ar}$), 126.8 (CH$_{Ar}$), 126.7 (CH$_{Ar}$), 56.0, 55.6 (CH$_{het}$), 54.2–49.7 (2 × COCH$_2$N), 49.2, 49.0 (CH), 47.8, 47.7 (NCH$_2$), 47.0 (NCH$_2$), 46.9 (NCH$_2$CH), 37.6, 37.1 (COCH$_2$CH), 32.7, 32.5 (NCH$_2$CH$_2$CH), 31.4 (NCH$_2$CH$_2$), 30.8 (NCH$_2$CH$_2$). HRMS (M + 1) calcd for C$_{39}$H$_{38}$^{35}Cl$_4$N$_4$O$_4$, 767.1720; found, 767.1735.

Synthesis of Compound 2 Analogues. The preparation of the first set of analogues (**2c**, **2d**, and **2e**) was carried out as follows. After all operations were carried out in solid phase, the polymer was drained and washed with with DCM (3 × 3 mL) and DMF (3 × 3 mL). Thus, three syringes were prepared with 250 mg of Rink amide resin (0.2 mmol) and treated separately with 3 mL of 20% piperidine in DMF. The resins were filtered and washed. Subse-

quently, resins were treated with a solution of bromoacetic acid (130 mg, 5 equiv) and DIC (145 μL, 5 equiv) in DMF (3 mL). The reaction mixtures were stirred for 2 min at 60 °C in a microwave reactor. After they were drained and washed, a solution of (tetrahydrofuran-2-yl)methanamine (98 μL, 5 equiv) and Et$_3$N (131 μL, 5 equiv) in 3 mL of DMF was added to the first resin and the suspension was stirred for 2 min at 90 °C under microwave activation. Another solution of butylamine (93 μL, 5 equiv) and Et$_3$N (131 μL, 5 equiv) in 3 mL of DMF was added to the second resin, and the suspension was stirred for 2 min at 90 °C under microwave activation. Finally, the third resin was treated with a solution of 2-(2-fluorophenyl)ethanamine (123 μL, 5 equiv) and Et$_3$N (131 μL, 5 equiv) in 3 mL of DMF and the suspension was stirred for 2 min at 90 °C under microwave activation. The supernatant of the three resins was removed, and the residue was drained and washed. Afterward, all resins were mixed into the same syringe and the subsequent steps were carried out together. The overall resin was treated with a solution of allyl maleate (440 mg, 5 equiv), HOBt (380 mg, 5 equiv), and DIC (436 μL, 5 equiv) in DCM/DMF (2:1, 5 mL). The reaction mixture was stirred at room temperature for 30 min and filtered, and the reaction was repeated under the same conditions. After the resin was drained and washed, a solution of 3,3-diphenylpropylamine (594 mg, 5 equiv) and Et$_3$N (395 μL, 5 equiv) in 6 mL of DMF was added to the resin and the suspension was stirred for 3 h at room temperature. The reaction was repeated overnight at the same temperature. The supernatant was removed, and the residue was drained and washed. Then the resin was treated with a solution of bromoacetic acid (391 mg, 5 equiv) and DIC (436 μL, 5 equiv) in DMF (6 mL). The reaction mixture was stirred for 2 min at 60 °C in a microwave reactor. The resin was drained and washed. A solution of 2,4-dichlorophenethylamine (425 μL, 5 equiv) and Et$_3$N (395 μL, 5 equiv) in 6 mL of DMF was added to the resin, and the suspension was stirred for 2 min at 90 °C under microwave activation. The supernatant was removed, and the residue was drained and washed. Then the resin was treated with Pd(PPh$_3$)$_4$ (65 mg, 0.1 equiv) and PhSiH$_3$ (693 μL, 10 equiv) in anhydrous DCM for 15 min at room temperature under an inert atmosphere. The supernatant was removed, and the residue was drained and washed. The final cyclization was promoted by treatment with PyBOP (440 mg, 1.5 equiv), HOBt (114 mg, 1.5 equiv), and DIEA (300 μL, 3 equiv) in DMF (6 mL). The reaction mixture was stirred at room temperature for 16 h and filtered. Finally, treatment of the resin (1013 g) with a mixture of 60:40:2 TFA/DCM/water released a crude reaction mixture containing the three target compounds. Solvents from the filtrate were removed by evaporation under reduced pressure followed by lyophilization. The residue obtained (286 mg) was characterized by analytical RP-HPLC and RP-HPLC−MS using aqueous acetonitrile gradient (20% CH_3CN → 80% CH_3CN, 20 min). Retention times of compounds were found to be 17.14 min for **2d**, 18.1 min for **2c**, and 19.0 min for **2e**. The crude reaction mixture was purified by semipreparative RP-HPLC using aqueous acetonitrile gradient (42% CH_3CN → 80% CH_3CN, 35 min) to give the desired products (yield 30–47%, ≥98% purity).

1-(3′,3′-Diphenylpropyl)-4-[2′-(2″,4″-dichlorophenyl)ethyl]-7-[*N*-(aminocarbonylmethyl)-*N*-[(tetrahydrofuran-2′-yl)methyl]aminocarbonyl]perhydro-1,4-diazepine-2,5-dione (2d):. HRMS (M + H)$^+$ calcd for C$_{35}$H$_{40}$^{35}Cl$_2$N$_4$O$_5$, 679.2449; found, 679.2443.

1-(3′,3′-Diphenylpropyl)-4-[2′-(2″,4″-dichlorophenyl)ethyl]-7-[*N*-(aminocarbonylmethyl)-*N*-(butyl)aminocarbonyl]perhydro-1,4-diazepine-2,5-dione (2c):. HRMS (M + H)$^+$ calcd for C$_{35}$H$_{40}$^{35}Cl$_2$N$_4$O$_4$, 651.2499; found, 651.2524.

1-(3′,3′-Diphenylpropyl)-4-[2′-(2″,4″-dichlorophenyl)ethyl]-7-[*N*-(aminocarbonylmethyl)-*N*-[2′-(2″-fluorophenyl)ethyl]aminocarbonyl]perhydro-1,4-diazepine-2,5-dione (2e):. HRMS (M + H)$^+$ calcd for C$_{39}$H$_{39}$^{35}Cl$_2$FN$_4$O$_4$, 717.2405; found, 717.2396.

The same procedure was carried out for the synthesis of the second and the third subset of compound **2** derivatives (second subset **2f**, **2g**, and **2h** and third subset **2a** and **2b**). Retention times for compounds were 16.49 min for **2f**, 20.91 min for **2g**, 21.55 min for **2h**, and 20.58 min for **2b**. The corresponding crude reaction

mixtures were purified as described above to yield the expected compounds in 30–45% yields and $\geq$98% purity).

1-(3′,3′-Diphenylpropyl)-4-[2′-(2″,4″-dichlorophenyl)ethyl]-7-[*N*-(aminocarbonylmethyl)-*N*-(2′-acetylaminoethyl)aminocarbonyl]perhydro-1,4-diazepine-2,5-dione (2f):. HRMS (M + H)$^+$ calcd for $C_{35}H_{39}{}^{35}Cl_2N_5O_5$, 680.2401; found, 680.2376.

1-(3′,3′-Diphenylpropyl)-4-[2′-(2″,4″-dichlorophenyl)ethyl]-7-[*N*-(aminocarbonylmethyl)-*N*-[2′-(2″-methoxyphenyl)ethyl]aminocarbonyl]perhydro-1,4-diazepine-2,5-dione (2g):. HRMS (M + H)$^+$ calcd for $C_{40}H_{42}{}^{35}Cl_2N_4O_5$, 729.2605; found, 729.2613.

1-(3′,3′-Diphenylpropyl)-4-[2′-(2″,4″-dichlorophenyl)ethyl]-7-[*N*-aminocarbonylmethyl-*N*-[2′-(4″-chlorophenyl)ethyl]aminocarbonyl]perhydro-1,4-diazepine-2,5-dione (2h):. HRMS (M + H)$^+$ calcd for $C_{39}H_{39}{}^{35}Cl_3N_4O_4$, 733.2110; found, 733.2084.

1-(3′,3′-Diphenylpropyl)-4-[2′-(2″,4″-dichlorophenyl)ethyl]-7-[*N*-(aminocarbonylmethyl)-*N*-(cyclopropyl)aminocarbonyl]perhydro-1,4-diazepine-2,5-dione (2b):. HRMS (M + H)$^+$ calcd for $C_{34}H_{36}{}^{35}Cl_2N_4O_4$, 635.2186; found, 635.2173.

1-(3′,3′-Diphenylpropyl)-4-[2′-(2″,4″-dichlorophenyl)ethyl]-7-[*N*-(aminocarbonylmethyl)-*N*-[2′-(4″-fluorophenyl)ethyl]aminocarbonyl]perhydro-1,4-diazepine-2,5-dione (2a):. HRMS (M + H)$^+$ calcd for $C_{39}H_{39}{}^{35}Cl_2FN_4O_4$, 717.2405; found, 717.2410.

Biological Assays. Cell Culture and Culture Conditions. The U937 human histiocytic lymphoma and the U-2 OS human osteosarcoma cell lines were obtained from the American Type Culture Collection (Rockville, MD). The U937 cells were grown in suspension in RPMI 1640 medium supplemented with 10% FCS and 2 mM L-glutamine. The Saos-2 human osteosarcoma cell line were kindly provided by Karin Vousden (Cancer Research U.K., Glasgow), and the HeLa human cervix adenocarcinoma cell lines were kindly provided by Jaime Font de Mora (CIPF, Valencia, Spain). The U-2 OS, Saos-2, HeLa, and A549 cells were grown in Dulbecco's modified Eagle's medium supplemented with 15% FCS and 2 mM L-glutamine in all cases except in Saos-2. Cells were maintained at 37 °C in an atmosphere of 5% carbon dioxide and 95% air and underwent passage twice weekly.

Culture of Neonatal Rat Cardiomyocytes and Hypoxic Conditions. Rat neonatal cardiomyocytes were prepared from ventricles of 1–2 days Wistar rats by a previously described method[34,36] with some modifications. Briefly, hearts were isolated, auricles were discarded, and ventricles were minced and digested with 2 mg/mL of collagenase type II for 1 h and subsequently with 1.2 U/mL dispase for 30 min with gently shaking. After two washes primary cultures were preplated for 90 min to eliminate contaminating fibroblasts. Hypoxia was induced by incubating the cardiomyocyte cultures in an atmosphere of 1% O_2. Experiment was performed three times with different breedings. Each procedure was repeated twice for two identically treated culture flasks.

MTT Cell Viability Assays.[37] Cells were cultured in sterile 96-well microtiter plates at a seeding density of 10^4, 3×10^3, 2.5×10^3, and 2×10^3 cells/well for Saos-2, U-2 OS, HeLa, and A549, respectively, and 2.5×10^3 and 4×10^3 cells/well in the case of U937, and they were allowed to set for 24 h. Doxycycline (2 μg/mL in PBS) for Saos-2 cells and doxorubicin in the cases of A549, HeLa, U-2 OS, and U937 at concentrations of 1, 1.5, 2, and 0.25 μg/mL in PBS, respectively, were then added, and after 30 min cells were treated with compounds (0.2 μm filter sterilized) at final concentrations of 1, 5, and 10 μM in the cases of PEN$-$1, TAT$-$1, and **2** and its derivatives, while PGA$-$1 was tested at concentrations of 20, 50, and 100 μM drug equivalents. Compounds were incubated for 19 h, and then MTT (20 μL of a 5 mg/mL solution) was added to each well. Cells were further incubated for 5 h (a total of 24 h of incubation with the inhibitors was therefore studied). In the next step, medium was removed, the precipitated formazan crystals were dissolved in optical grade DMSO (100 μL), and plates were read at 570 nm using a Wallac 1420 workstation.

Caspase Activation Assays in Cellular Models (DEVDase Activity). Cell extracts were prepared from cells seeded in 3.5 cm diameter plates at seeding densities of 2×10^5 cells per plate in the case of Saos-2, 3×10^5 and 3.5×10^5 cells per plate for HeLa and U-2 OS, and 4×10^5 and 4.5×10^5 cells per plate for U937,

and they were allowed to set for 24 h.[13] Then cells were treated with doxycycline (2 μg/mL in PBS) for Saos-2 cells and doxorubicin in the cases of HeLa, U-2 OS, and U937 at concentrations of 2, 2.5, and 0.25 μg/mL in PBS, respectively. After 30 min, PEN$-$1 and compound **2** derivatives at 5 μM and PGA$-$1 at 50 and 100 μM drug equivalents were added. Cells were harvested after 24, 48, and 72 h of incubation and pellets resuspended in 30 μL of extraction buffer (50 mM PIPES, 50 mM KCl, 5 mM EDTA, 2 mM $MgCl_2$, 2 mM DTT supplemented with protease inhibitor cocktail from Sigma) and kept on ice for 5 min. Once pellets were frozen and thawed three times, cell lysates were centrifuged at 14 000 rpm for 5 min and supernatants were collected. Quantification of total protein concentration from these cell extracts was performed using the bicinchoninic acid method. Aliquots were prepared at the same concentration, and afterward they were mixed with 200 μL of caspases assay buffer (PBS, 10% glycerol, 0.1 mM EDTA, 2 mM DTT) containing 20 μM Ac-DEVD-afc. Caspase activity was continuously monitored following the release of fluorescent afc at 37 °C using a Wallac 1420 Workstation (λ_{exc}= 400 nm; λ_{em}= 508 nm). DEVDase activity was expressed as the increase of relative fluorescence units per minute (ΔFU/min).

Evaluation of Cellular Apoptosis by Flow Cytometry Analysis. Saos-2 and U937 cells were seeded in six-well plates at a seeding density of 2×10^5 and 4×10^5 cells per plate, respectively. Cells were treated with doxycycline (2 μg/mL in PBS) and doxycycline plus PGA$-$1 (50 μM drug equivalent) for Saos-2 or doxorubicin (0.25 μg/mL in H_2O) and doxorubicin plus PGA$-$1 in the case of U937 for 24, 48, and 72 h. Apoptosis was analyzed by flow cytometry by determining the changes in cell forward/side scatter and through the determination of phosphatidylserine (PS) exposure and mitochondrial membrane potential ($\Delta\Psi_m$) loss with Annexin V-FITC and 3,3-dihexyloxacarbocyanine iodide (Di-OC_6(3)), respectively. Necrotic cell death was distinguished from apoptotic using propidium iodide (PI) by co-incubation either with Annexin V-FITC or with $DiOC_6$(3). FL1 detector was used to analyze Annexin V-FITC binding or $DiOC_6$(3) accumulation (λ_{exc} = 488 nm; λ_{em} = 530 nm), and PI staining was followed by signal detector FL3 (λ_{exc} = 530 nm; λ_{em} = 617 nm). For adherent cells, first these were gently trypsinized and washed twice with cold PBS. Then cells were resuspended in 1× binding buffer (10 mM Hepes/NaOH (pH 7.4), 140 mM NaCl, 2.5 mM $CaCl_2$) at a concentration of 1×10^6 cells/mL. After the transfer of 100 μL of the cell solutions (1×10^5 cells) to a 5 mL culture tube, two different staining protocols were followed: (i) 5 μL of annexin V-FITC and 5 μL of PI (ready-to-use solutions from the apoptosis detection kit) were added to the cell solutions. Cells were gently vortexed and incubated for 15 min at room temperature in the dark. (ii) An amount of 5 μL of 100 nM $DiOC_6$(3) in PBS was added to the solution, and cells were incubated for 30 min at 37 °C. Then 5 μL of PI (ready-to-use solutions from the apoptosis detection kit) was also added and incubated for further 15 min at room temperature in the dark. The highly fluorescent population was considered viable cells, and the dull population represented apoptotic cells. Prior to flow cytometry analysis, an amount of 400 μL of 1× binding buffer was added in all cases to each tube.

Immunohistochemistry. Cardiomyocytes were fixed in 2% paraformaldehyde (PFA). Immunohistochemistry was performed with antibodies against caspase-3 (1:100) and anti-α-actinine (sacomeric) (1:800) followed by detection with secondary antibodies coupled to either cyanine or FITC.

Statistical Analysis. Data are expressed as the mean ± standard error. Student *t* tests were performed, and mean values were considered statistically significant when *p* values less than 0.05 were obtained.

Supporting Information Available: HRMS spectra of key target compounds. This material is available free of charge via the Internet at http://pubs.acs.org.

References

(1) Fesik, S. W. Promoting apoptosis as a strategy for cancer drug discovery. *Nat. Rev. Cancer* **2005**, *5*, 876–885.

(2) Nencioni, A.; Grunebach, F.; Patrone, F.; Ballestrero, A.; Brossart, P. The proteasome and its inhibitors in immune regulation and immune disorders. *Crit. Rev. Immunol.* **2006**, *26*, 487–497.

(3) Fischer, U.; Schulze-Osthoff, K. New approaches and therapeutics targeting apoptosis in disease. *Pharmacol. Rev.* **2005**, *57*, 187–215.

(4) Takemura, G.; Fujiwara, H. Morphological aspects of apoptosis in heart diseases. *J. Cell. Mol. Med.* **2006**, *10*, 56–75.

(5) Mattson, M. P.; Kroemer, G. Mitochondria in cell death: novel targets for neuroprotection and cardioprotection. *Trends Mol. Med.* **2003**, *9*, 196–205.

(6) Siegel, R. M. Caspases at the crossroads of immune-cell life and death. *Nat. Rev. Immunol.* **2006**, *6*, 308–317.

(7) Chai, J. J.; Du, C. Y.; Wu, J. W.; Kyin, S.; Wang, X. D.; et al. Structural and biochemical basis of apoptotic activation by Smac/DIABLO. *Nature* **2000**, *406*, 855–862.

(8) Li, P.; Nijhawan, D.; Budihardjo, I.; Srinivasula, S. M.; Ahmad, M.; et al. Cytochrome *c* and dATP-dependent formation of Apaf-1/caspase-9 complex initiates an apoptotic protease cascade. *Cell* **1997**, *91*, 479–489.

(9) Martin, A. G.; Nguyen, J.; Wells, J. A.; Fearnhead, H. O. Apo cytochrome *c* inhibits caspases by preventing apoptosome formation. *Biochem. Biophys. Res. Commun.* **2004**, *319*, 944–950.

(10) Schafer, Z. T.; Kornbluth, S. The apoptosome: physiological, developmental, and pathological modes of regulation. *Dev. Cell* **2006**, *10*, 549–561.

(11) Mochizuki, H.; Hayakawa, H.; Migita, M.; Shibata, M.; Tanaka, R.; et al. An AAV-derived Apaf-1 dominant negative inhibitor prevents MPTP toxicity as antiapoptotic gene therapy for Parkinson's disease. *Proc. Natl. Acad. Sci. U.S.A.* **2001**, *98*, 10918–10923.

(12) Cao, G. D.; Xiao, M.; Sun, F. Y.; Xiao, X.; Pei, W.; et al. Cloning of a novel Apaf-1-interacting protein: a potent suppressor of apoptosis and ischemic neuronal cell death. *J. Neurosci.* **2004**, *24*, 6189–6201.

(13) Malet, G.; Martín, A. G.; Orzáez, M.; Vicent, M. J.; Masip, I.; et al. Small molecule inhibitors of Apaf-1-related caspase-3/-9 activation that control mitochondrial-dependent apoptosis. *Cell Death Differ.* **2006**, *13*, 1523–1532.

(14) Orzaez, M.; Mondragon, L.; Marzo, I.; Sanclimens, G.; Messeguer, A.; et al. Conjugation of a novel Apaf-1 inhibitor to peptide-based cell-membrane transporters: effective methods to improve inhibition of mitochondria-mediated apoptosis. *Peptides* **2007**, *28*, 958–968.

(15) Vicent, M. J.; Pérez-Payá, E. Poly-L-glutamic acid (PGA) aided inhibitors of apoptotic protease activating factor 1 (Apaf-1): an antiapoptotic polymeric nanomedicine. *J. Med. Chem.* **2006**, *49*, 3763–3765.

(16) Tsujimoto, Y. Role of Bcl-2 family proteins in apoptosis: apoptosomes or mitochondria. *Genes Cells* **1998**, *3*, 697–707.

(17) Chan, S. L.; Yu, V. C. Proteins of the bcl-2 family in apoptosis signalling: from mechanistic insights to therapeutic opportunities. *Clin. Exp. Pharmacol. Physiol.* **2004**, *31*, 119–128.

(18) Duncan, R. Drug polymer conjugates—potential for improved chemotherapy. *Anti-Cancer Drugs* **1992**, *3*, 175–210.

(19) Lademann, U.; Cain, K.; Gyrd-Hansen, M.; Brown, D.; Peters, D.; et al. Diarylurea compounds inhibit caspase activation by preventing the formation of the active 700-kilodalton apoptosome complex. *Mol. Cell. Biol.* **2003**, *23*, 7829–7837.

(20) Nguyen, J. T.; Wells, J. A. Direct activation of the apoptosis machinery as a mechanism to target cancer cells. *Proc. Natl. Acad. Sci. U.S.A.* **2003**, *100*, 7533–7538.

(21) Bras, M.; Queenan, B.; Susin, S. A. Programmed cell death via mitochondria: different modes of dying. *Biochemistry (Moscow)* **2005**, *70*, 231–239.

(22) Green, D. R. Apoptotic pathways: ten minutes to dead. *Cell* **2005**, *121*, 671–674.

(23) Martinou, I.; Desagher, S.; Eskes, R.; Antonsson, B.; Andre, E.; et al. The release of cytochrome *c* from mitochondria during apoptosis of NGF-deprived sympathetic neurons is a reversible event. *J. Cell Biol.* **1999**, *144*, 883–889.

(24) Seye, C. I.; Knaapen, M. W. M.; Daret, D.; Desgranges, C.; Herman, A. G. 7-Ketocholesterol induces reversible cytochrome *c* release in smooth muscle cells in absence of mitochondrial swelling. *Cardiovasc. Res.* **2004**, *64*, 144–153.

(25) Anversa, P.; Cheng, W.; Liu, Y.; Leri, A.; Redaelli, G.; et al. Apoptosis and myocardial infarction. *Basic Res. Cardiol.* **1998**, *93*, 8–12.

(26) Itoh, G.; Tamura, J.; Suzuki, M.; Suzuki, Y.; Ikeda, H. DNA fragmentation of human infarcted myocardial cells demonstrated by the nick end labeling method and DNA agarose gel electrophoresis. *Am. J. Pathol.* **1995**, *146*, 1325–1331.

(27) Schwarz, K.; Simonis, G.; Yu, X.; Wiedemann, S.; Strasser, R. H. Apoptosis at a distance: remote activation of caspase-3 occurs early after myocardial infarction. *Mol. Cell. Biochem.* **2006**, *281*, 45–54.

(28) Fliss, H.; Gattinger, D. Apoptosis in ischemic and reperfused rat myocardium. *Circ. Res.* **1996**, *79*, 949–956.

(29) Gottlieb, R. A.; Engler, R. L. Apoptosis in myocardial ischemia-reperfusion. *Ann. N.Y. Acad. Sci.* **1999**, *874*, 412–426.

(30) Wang, G. W.; Zhou, Z.; Klein, J. B.; Kang, Y. J. Inhibition of hypoxia/reoxygenation-induced apoptosis in metallothionein-overexpressing cardiomyocytes. *Am. J. Physiol.: Heart Circ. Physiol.* **2001**, *280*, H2292–H2299.

(31) Ferrari, R. Metabolic disturbances during myocardial ischemia and reperfusion. *Am. J. Cardiol.* **1995**, *76*, 17B–24B.

(32) Lucas, D. T.; Szweda, L. I. Declines in mitochondrial respiration during cardiac reperfusion: age-dependent inactivation of alpha-ketoglutarate dehydrogenase. *Proc. Natl. Acad. Sci. U.S.A.* **1999**, *96*, 6689–6693.

(33) Wencker, D.; Chandra, M.; Nguyen, K.; Miao, W. F.; Garantziotis, S.; et al. A mechanistic role for cardiac myocyte apoptosis in heart failure. *J. Clin. Invest.* **2003**, *111*, 1497–1504.

(34) Hayakawa, Y.; Chandra, M.; Miao, W. F.; Shirani, J.; Brown, J. H.; et al. Inhibition of cardiac myocyte apoptosis improves cardiac function and abolishes mortality in the peripartum cardiomyopathy of G alpha q transgenic mice. *Circulation.* **2003**, *108*, 3036–3041.

(35) Masip, I.; Cortes, N.; Abad, M. J.; Guardiola, M.; Perez-Paya, E.; et al. Design and synthesis of an optimized positional scanning library of peptoids: identification of novel multidrug resistance reversal agents. *Bioorg. Med. Chem.* **2005**, *13*, 1923–1929.

(36) Kijima, K.; Matsubara, H.; Murasawa, S.; Maruyama, K.; Mori, Y.; et al. Mechanical stretch induces enhanced expression of angiotensin II receptor subtypes in neonatal rat cardiac myocytes. *Circ. Res.* **1996**, *79*, 887–897.

(37) Sgouras, D.; Duncan, R. Methods for the evaluation of biocompatibility of soluble synthetic-polymers which have potential for bio-medical use. 1. Use of the tetrazolium-based colorimetric assay (Mtt) as a preliminary screen for evaluation of invitro cytotoxicity. *J. Mater. Sci.: Mater. Med.* **1990**, *1*, 61–68.

JM701195J